

Raman Scattering from Magnetic Excitations in coupled Spin Ladders

R. Citro^a and E. Orignac^b

^a*Dipartimento di Scienze Fisiche "E.R. Caianiello",*

University of Salerno and Unità INFM of Salerno, Baronissi (Sa), Italy

^b*Laboratoire de Physique Théorique, CNRS UMR 8549,*

Ecole Normale Supérieure, 24 Rue Lhomond 75231 Paris Cedex 05, France

(November 13, 2018)

We consider Raman scattering of coupled two leg spin ladders in the Fleury-Loudon regime. We derive the dependence of the intensity with polarization of the incoming light and temperature and discuss the effect of interaction of the elementary excitations on the shape of the spectrum. We show that Raman scattering spectrum is sensitive to the effective dimensionality of the coupled ladder system, making Raman scattering useful to discriminate true ladder systems from quasi two dimensional spin gap systems.

PACS numbers: 72.12.Di 87.64.Je 75.10.Jm

The study of spin ladder compounds¹ has become a subject of intense theoretical and experimental activity² in the recent years. Insulating two leg spin-ladder compounds present a spin gap state that has been probed experimentally by thermodynamic (specific heat and magnetic susceptibility) measurements as well as dynamical measurements such as neutron scattering or NMR. Another technique to study the dynamics of magnetic excitations in low dimensional antiferromagnets is Raman scattering. This technique has been used in particular to probe spin 1/2 chains³, spin 1 chains⁴ and spin Peierls systems⁵⁻⁸. The extended interest towards this experimental technique is due to its sensitivity to singlet excitations, that render it complementary to neutron diffraction experiments. There exists at present a certain amount of literature on the theory of Raman scattering from dimerized spin chains, both analytical^{9,10} and numerical¹¹ in relation to experiments on Spin-Peierls compounds⁵⁻⁸. In the case of spin ladder materials, although there are quite a few experimental investigations¹²⁻¹⁶ by Raman scattering, there is a scarcity of theoretical results on this subject. While some numerical calculations are available to describe the experimental data¹⁷, no analytical expressions of the Raman intensity for $2n$ -legged spin-1/2 ladders existed. In all the theoretical work on spin ladders, the analysis of magnetic Raman scattering is based on the Fleury-Loudon Hamiltonian¹⁹⁻²¹, that describes the interaction of photons with magnetic excitations. This limits the investigations to the non-resonant regime²¹. In a previous report¹⁸, we have derived the relevant expressions for two leg ladders with weak and strong interladder coupling. In our report¹⁸, we found that for weak coupling case the Majorana fermions description of the spin ladder²² lead to a cusp in the Raman intensity at twice the gap. This was in disagreement with experiments that show a peak rather than a cusp in the Raman intensity for a frequency twice the gap. On the other hand, in the strong coupling case, the Bond Operator Technique²³⁻²⁵ (BOT) predicted correctly the presence of the peak at

twice the gap. This suggests that the strong coupling description is more adequate to describe Raman scattering experiments in real spin ladder systems. In our report, some important aspects of Raman scattering in spin ladder were not considered. First, we restricted ourselves to zero temperature. However, the spin gap is temperature dependent and thus temperature should modify the Raman intensity. A second aspect that was not considered is the effect of interactions between the magnetic excitations. Such interactions break the coherence that gives rise to the peaks and it is important to understand how they modify the ideal spectrum of Ref. 18. A last aspect is the influence of interladder excitations. There are spin ladder materials^{26,27} in which the interladder coupling is by no means negligible such as KCuCl_3 or $\text{VO}_2\text{P}_2\text{O}_7$. This affects strongly the neutron scattering intensity compared to the one of a single ladder. This two-dimensionality should also affect the Raman spectrum. Understanding how the Raman intensity is affected by dimensionality is important to discriminate a one-dimensional from a two-dimensional compound. A possible application could be to the CuHpCl compound for which there exists some evidence of two dimensional behavior²⁸ (See however Refs. 29-31).

In the present paper we deal with the calculation of the Raman scattering cross section of coupled spin ladders. After recalling some basic results on the Fleury-Loudon theory of magnetic Raman scattering, and the Bond Operator Technique^{24,25} (BOT) we give the general derivation of the Raman operator for coupled ladders in Sec. I. In Sec. II we give an expanded discussion of the two leg Heisenberg ladder¹⁸. We discuss the temperature dependence of the Raman intensity of the ladder. We also consider the effect of interactions on the peaks in the Raman spectrum and derive a scaling form of the intensity valid in the vicinity of the edges of the Raman spectrum. Having illustrated the technique on and the physics on the simple isolated ladder case, we turn in Sec. III B 2 to the case of coupled ladders. First, we consider a system of two coupled ladders, for which the Raman spectrum

presents four peaks. The influence of temperature and interactions on the spectrum is the same as in the case of the isolated ladder. Then, we consider the case of a two dimensional array of ladders. We show that the spectrum of this system is markedly different from that of the isolated ladder, and discuss the effect of the interactions of magnetic excitations on the singularities of the two-dimensional spectrum.

I. THE LOUDON-FLEURY THEORY FOR THE PERIODIC ARRAY OF LADDERS

We consider a periodic array of single-rung two-legged Heisenberg ladders (shown in Fig.1) whose Hamiltonian is

$$H = \sum_{i,j} (J_{\parallel} \mathbf{S}_{i,j} \cdot \mathbf{S}_{i+1,j} + J_{\perp} \mathbf{S}_{i,2j} \cdot \mathbf{S}_{i,2j+1} + J'_{\perp} \mathbf{S}_{i,2j+1} \cdot \mathbf{S}_{i,2j+2}), \quad (1)$$

where $J_{\parallel} = \lambda J_{\perp}$ is the interaction along the legs of the ladder, J_{\perp} is the rung interaction and $J'_{\perp} = \lambda' J_{\perp}$ is the interladder coupling. The index i and j run along the leg and rung direction respectively. In the limit $\lambda' = 0$ the Hamiltonian reduces to a sum of independent single-rung ladders, while in the limit $\lambda = \lambda' = 0$ (strong-coupling) the Hamiltonian reduces to a sum over independent two spin rungs. In this paper we are interested in the regime $\lambda' < \lambda < 1$.

The interaction of light with the antiferromagnetic fluctuations is described by Loudon-Fleury's^{19,20} photon-induced super-exchange operator

$$H_R = \sum_{\mathbf{l}, \mathbf{l}'} \gamma_{\mathbf{l}\mathbf{l}'} (\mathbf{E}_{\mathbf{l}} \cdot \delta_{\mathbf{l}\mathbf{l}'}) (\mathbf{E}_{\mathbf{S}} \cdot \delta_{\mathbf{l}\mathbf{l}'}) \mathbf{S}_{\mathbf{l}} \cdot \mathbf{S}_{\mathbf{l}'} \quad (2)$$

where $\mathbf{E}_{\mathbf{l}}(\mathbf{E}_{\mathbf{S}})$ are the incident (scattered) electric field vectors of photon, and $\delta_{\mathbf{l}\mathbf{l}'}$ is a unit vector connecting the lattice sites \mathbf{l} and \mathbf{l}' , at which the spins $\mathbf{S}_{\mathbf{l}}$ and $\mathbf{S}_{\mathbf{l}'}$ are located. A derivation of (2) starting from the Hubbard Hamiltonian can be found in Ref. 21.

The Raman cross section^{32,33} can be expressed in terms of the retarded Raman response function as:

$$\frac{d^2\sigma}{d\Omega d\omega_2} = \frac{\omega_1 \omega_2^3}{2\pi c^4 V} \frac{n_2}{n_1} \frac{1}{1 - e^{-\beta\hbar\omega}} \text{Im}\chi_R(\omega) \quad (3)$$

ω_1 and ω_2 are the frequencies of the incoming and scattered radiation, respectively, $\omega = \omega_2 - \omega_1$, n_1 and n_2 are the refractive indices of the material at frequency respectively ω_1 and ω_2 . V is the volume of the crystal and c the velocity of light. The retarded linear response function $\chi_R(\omega)$ is defined as:

$$\chi_R^{ret}(\omega) = \frac{i}{\hbar} \int_0^{\infty} e^{i(\omega+i0)t} \text{Tr} \{ Z^{-1} e^{-\beta H} [H_R(t), H_R(0)] \}, \quad (4)$$

where $Z = \text{Tr} e^{-\beta H}$ and H_R is the Loudon-Fleury Hamiltonian (2).

By inserting the resolution of identity in (4), the Raman intensity can be written as

$$\frac{d^2\sigma}{d\Omega d\omega_2} \propto \frac{1}{\hbar} \frac{1}{Z} \sum_{n,m} e^{-\beta E_n} |\langle \Psi_n | H_R | \Psi_m \rangle|^2 \delta(\omega - (E_n - E_m)/\hbar), \quad (5)$$

where $|\Psi_{n(m)}\rangle$ are eigenstates with energies $E_{n(m)}$. Such formula can be easily interpreted as a Fermi golden rule averaged over the Boltzmann weight. To obtain informations on two-magnons scattering processes we should perform a symmetry analysis of the matrix elements appearing in (5), and discuss selection rules. Since the spin ladder Hamiltonian is invariant under translation along the legs, SU(2) rotation, and mirror along the the leg direction, an eigenstate should be characterized by a (lattice) momentum defined modulo $2\pi/a$ (where a is the lattice spacing), a spin and its parity under leg exchange. The Raman operator defined in (2) is rotationally and translationally invariant, and still invariant under leg exchange. As a result, the selection rules impose that the states $|\Psi_n\rangle$ and $|\Psi_m\rangle$ have the same spin, momentum and parity under leg exchange. This implies in particular that at $T = 0$, transitions will only take place to states of total momentum zero, spin zero and same parity as the ground state.

To obtain an expression of the Raman Hamiltonian more adapted to perform the calculations, we introduce a coordinate system (\hat{x}, \hat{y}) where \hat{x} is parallel to the chain direction and \hat{y} is parallel to the rung direction. In this coordinate system, we have $\mathbf{l} = i\hat{x} + j\hat{y} = (i, j)$, $\mathbf{E}_{\mathbf{l}} = E_{\mathbf{l}}(\cos\theta_{\mathbf{l}}\hat{x} + \sin\theta_{\mathbf{l}}\hat{y})$ and $\mathbf{E}_{\mathbf{S}} = E_{\mathbf{S}}(\cos\theta_{\mathbf{S}}\hat{x} + \sin\theta_{\mathbf{S}}\hat{y})$. We define $\gamma_{\parallel} = \gamma_{(i,j),(i+1,j)}$, $\gamma_{\perp} = \gamma_{(i,2j),(i,2j+1)}$ and $\gamma'_{\perp} = \gamma_{(i,2j+1),(i,2j+2)}$. The expression of the Raman operator becomes:

$$H_R = E_{\mathbf{l}} E_{\mathbf{S}} \cos\theta_{\mathbf{S}} \cos\theta_{\mathbf{l}} \gamma_{\parallel} \sum_{i,j} \mathbf{S}_{i,j} \cdot \mathbf{S}_{i+1,j} + E_{\mathbf{l}} E_{\mathbf{S}} \sin\theta_{\mathbf{l}} \sin\theta_{\mathbf{S}} \times \left(\gamma_{\perp} \sum_{i,j} \mathbf{S}_{i,2j} \cdot \mathbf{S}_{i,2j+1} + \gamma'_{\perp} \sum_{i,j} \mathbf{S}_{i,2j+1} \cdot \mathbf{S}_{i,2j+2} \right) \quad (6)$$

This expression can be simplified using the form of the full Hamiltonian. One has:

$$H_R = \frac{\gamma'_{\perp}}{J'_{\perp}} E_{\mathbf{l}} E_{\mathbf{S}} \sin\theta_{\mathbf{l}} \sin\theta_{\mathbf{S}} H + E_{\mathbf{l}} E_{\mathbf{S}} \left(\gamma_{\parallel} \cos\theta_{\mathbf{S}} \cos\theta_{\mathbf{l}} - \frac{\gamma'_{\perp} J_{\parallel}}{J'_{\perp}} \sin\theta_{\mathbf{l}} \sin\theta_{\mathbf{S}} \right) \sum_{i,j} \mathbf{S}_{i,j} \cdot \mathbf{S}_{i+1,j} + E_{\mathbf{l}} E_{\mathbf{S}} \sin\theta_{\mathbf{l}} \sin\theta_{\mathbf{S}} \left(\gamma_{\perp} - \frac{\gamma'_{\perp} J_{\perp}}{J'_{\perp}} \right) \sum_{i,j} \mathbf{S}_{i,2j} \cdot \mathbf{S}_{i,2j+1} \quad (7)$$

The part of H_R proportional to H gives no contribution to the response functions.

In the case of a single ladder, $J'_\perp = 0$ and the simplified form of H_R is:

$$H_R^{sl} = \left(\gamma_\parallel \cos \theta_I \cos \theta_S - \frac{\gamma_\perp J_\parallel}{J_\perp} \sin \theta_I \sin \theta_S \right) \times E_I E_S \sum_{i,j} \sum_{i,j} \mathbf{S}_{i,j} \cdot \mathbf{S}_{i+1,j} \quad (8)$$

Some remarks on the coefficients γ_α , ($\alpha = \parallel, \perp$) are in order here. According to perturbative calculations²¹ for a half filled Hubbard ladder, one should have

$$\gamma_\perp / J_\perp = \gamma'_\perp / J'_\perp = \gamma_\parallel / J_\parallel. \quad (9)$$

With this relation, (8) is recovered when taking the limit $J'_\perp \rightarrow 0$ in (7). In such case, the simplified form of the Raman Hamiltonian is:

$$H_R = \gamma_\parallel E_I E_S \cos(\theta_I + \theta_S) \sum_{i,j} \mathbf{S}_{i,j} \cdot \mathbf{S}_{i+1,j} \quad (10)$$

This form has been previously obtained in Ref. 34. It leads to the same Raman intensity for $\theta_I = \theta_S = 0$ and $\theta_I = \theta_S = \pi/2$ in disagreement with experimental data³⁴. It was shown that treating the γ 's as phenomenological coefficients and assuming $\gamma_\alpha \propto \sqrt{J_\alpha}$ lead to better agreement with experiments³⁴. In the following, we will treat the γ 's as phenomenological coefficients and then specialize to the simplified expression that result when (9) is assumed.

To analyze the Raman susceptibility, we use the Bond Operator Representation (BOT)^{24,23} of quantum $S=1/2$ spins used by Gopalan, Rice and Sigris²⁵ in their mean field approach to spin ladders. In this representation, one starts from weakly coupled rungs, i.e. $\lambda = 0$, and introduces on each rung a singlet s^\dagger and three triplets t_α^\dagger ($\alpha = x, y, z$) boson creation operators, that span the Hilbert space of a single rung when acting on a vacuum state. Since the rung can be in either the singlet or one of the triplet states, the condition :

$$s^\dagger s + \sum_\alpha t_\alpha^\dagger t_\alpha = 1 \quad (11)$$

has to be satisfied by the physical states. The representation of the spins $\mathbf{S}_{i,2j}$ and $\mathbf{S}_{i,2j+1}$ in terms of these singlet and triplet operators, is derived in Ref.^{24,25}. It reads:

$$S_{i,2j}^\alpha = \frac{1}{2} (s^\dagger t_\alpha + t_\alpha^\dagger s - i \epsilon_{\alpha\beta\gamma} t_\beta^\dagger t_\gamma)_{i,2j} \quad (12)$$

$$S_{i,2j+1}^\alpha = \frac{1}{2} (-s^\dagger t_\alpha - t_\alpha^\dagger s - i \epsilon_{\alpha\beta\gamma} t_\beta^\dagger t_\gamma)_{i,2j} \quad (13)$$

The Hamiltonian Eq. (1) can be rewritten in the BOT as:

$$H = \left(\frac{J_\perp}{4} - \mu \right) \sum_{i,j,\alpha} t_{i,j,\alpha}^\dagger t_{i,j,\alpha} + \frac{\lambda J_\perp s^2}{2} \sum_{i,j,\alpha} (t_{i,j,\alpha} + t_{i,j,\alpha}^\dagger) (t_{i+1,j,\alpha} + t_{i+1,j,\alpha}^\dagger)$$

$$- \lambda' J_\perp \frac{s^2}{4} \sum_{i,j=1,2} (t_{i,j,\alpha} + t_{i,j,\alpha}^\dagger) (t_{i,j+1,\alpha} + t_{i,j+1,\alpha}^\dagger) + \sum_{i,j} \left(-\frac{3}{4} J_\perp s^2 - \mu s^2 + \mu \right) + \text{quartic terms.} \quad (14)$$

The quartic terms in t, t^\dagger in Eq. (14) describe interactions between triplet excitations. Their explicit form will not be needed here.

Substituting the operator representation of spins Eq. (13) into the Raman operator for coupled ladders Eq. (7), one ends up with the following expression:

$$H_R = E_I E_S \left(\gamma_\parallel \cos \theta_S \cos \theta_I - \frac{\gamma'_\perp J_\parallel}{J'_\perp} \sin \theta_I \sin \theta_S \right) \times \frac{s^2}{4} \sum_{i,j,\alpha} (t_{i+1,2j,\alpha}^\dagger + t_{i+1,2j,\alpha}) (t_{i,2j,\alpha}^\dagger + t_{i,2j,\alpha}) + E_I E_S \sin \theta_I \sin \theta_S \left(\gamma_\perp - \frac{\gamma'_\perp J_\perp}{J'_\perp} \right) \sum_{i,j,\alpha} \frac{1}{4} t_{i,2j,\alpha}^\dagger t_{i,2j,\alpha} \quad (15)$$

In Fourier space, this expression becomes:

$$H_R = \frac{E_I E_S}{4} \sum_{\mathbf{k},\alpha} \left(A_{\mathbf{k}} t_{\mathbf{k},\alpha}^\dagger t_{\mathbf{k},\alpha} + B_{\mathbf{k}} (e^{ik_x a} t_{\mathbf{k},\alpha}^\dagger t_{-\mathbf{k},\alpha}^\dagger + \text{H. c.}) \right) \quad (16)$$

where:

$$A_{\mathbf{k}} = \left(\gamma_\perp - \frac{\gamma'_\perp J_\perp}{J'_\perp} \right) \sin \theta_I \sin \theta_S + 2s^2 \cos(k_x a) \left(\gamma_\parallel \cos \theta_I \cos \theta_S - \frac{\gamma'_\perp J_\parallel}{J'_\perp} \sin \theta_I \sin \theta_S \right) B_{\mathbf{k}} = s^2 \gamma_\parallel \cos \theta_I \cos \theta_S - s^2 \frac{\gamma'_\perp J_\parallel}{J'_\perp} \sin \theta_I \sin \theta_S \quad (17)$$

In particular, if $\gamma_\parallel / J_\parallel = \gamma_\perp / J_\perp = \gamma'_\perp / J'_\perp$, we get the following relation between the coefficients

$$A_{\mathbf{k}} = 2B_{\mathbf{k}} \cos(k_x a) = 2s^2 \gamma_\parallel \cos k_x a \cos(\theta_I + \theta_S). \quad (18)$$

The above expressions will be used in the following of the paper to predict the Raman intensity.

II. THE SINGLE RUNG LADDER

A. Mean field theory

We start by considering a single ladder of two strongly coupled antiferromagnetic $S = 1/2$ Heisenberg chains, whose Hamiltonian is

$$H = J_\parallel \sum_i (\mathbf{S}_{1,i} \mathbf{S}_{1,i+1} + \mathbf{S}_{2,i} \mathbf{S}_{2,i+1}) + J_\perp \sum_i \mathbf{S}_{1,i} \cdot \mathbf{S}_{2,i} \quad (19)$$

where $J_{\parallel} = \lambda J_{\perp} > 0$ and $J_{\perp} > 0$ denotes the intra- and inter-chain antiferromagnetic interactions, respectively. Substituting the BOT operator representation of spins (13) into the original Hamiltonian, one ends up with an Hamiltonian quartic in boson fields. Treating the singlet operator in a mean field approximation and neglecting interactions among the triplets, one obtains the following Hamiltonian quadratic in triplet operators²⁵:

$$H_{MF} = \left(\frac{J_{\perp}}{4} - \mu\right) \sum_{i,\alpha} t_{i,\alpha}^{\dagger} t_{i,\alpha} + \frac{J_S^2}{2} \sum_{i,\alpha} (t_{i,\alpha}^{\dagger} + t_{i,\alpha})(t_{i+1,\alpha}^{\dagger} + t_{i+1,\alpha}). \quad (20)$$

The chemical potential term μ guarantees that the condition (11) is satisfied on average. The parameters μ and s are determined in a self-consistent way by the minimization of the free-energy. The self consistent equations to be solved are:

$$\begin{aligned} \left(s^2 - \frac{3}{2}\right) + \int_0^{\pi} \frac{dk}{4\pi} \coth\left(\frac{\beta\omega_k}{2}\right) \left[\sqrt{1+d\cos k} + \frac{1}{\sqrt{1+d\cos k}}\right] &= 0 \\ \left(\frac{3}{2} + 2\frac{\mu}{J_{\perp}}\right) + \frac{4\lambda}{d} \int_0^{\pi} \frac{dk}{4\pi} \coth\left(\frac{\beta\omega_k}{2}\right) \left[\frac{1}{\sqrt{1+d\cos k}} - \sqrt{1+d\cos k}\right] &= 0. \end{aligned} \quad (21)$$

where

$$d = \frac{2\lambda s^2}{\left(\frac{1}{4} - \frac{\mu}{J_{\perp}}\right)}. \quad (22)$$

After some simple manipulations, from equations (21) we obtain the following equation for d

$$d = \lambda \left[3 - \int_0^{\pi} \frac{dk}{\pi} \frac{\coth\left(\frac{\beta\omega_k}{2}\right)}{\sqrt{1+d\cos k}} \right]. \quad (23)$$

When this equation is combined with the first equation in (21), we can solve them numerically to obtain s^2 and d . Only in the zero temperature limit these equations decouple completely and reduce to the equations (2.19) of Ref. 25. For the purpose of this paper, i.e. the analysis of the Raman intensity, we discuss the temperature dependence of the singlet order parameter $s(T)$ and $d(T)$. The numerical analysis shows (see Fig.(3)) that at high enough temperature s is very small and increases as temperature is lowered. Such behavior is expected since at high enough temperature bosons cannot condense. In this high temperature regime where $s(T) = 0$ the mean-field Hamiltonian (20) commutes with the Raman operator, leading to zero Raman intensity from magnetic scattering. For low enough temperature, $s(T) \neq 0$ and a Raman signal appears. As temperature is lowered, the

bandwidth of triplet excitations increases and the width of the magnetic Raman scattering increases. Let us point out that the mean field calculation of $s(T)$ is valid only for a low density of triplets i. e. for low enough temperature. At high temperature, the triplet-triplet interactions cannot be neglected. However, the mean-field theory gives nevertheless a qualitatively correct picture of the development of Raman intensity. The Raman intensity (see Appendix) is given by:

$$\begin{aligned} \text{Im}\chi_R(\omega) = C^2(\theta_I, \theta_S) \int dk \coth\left(\frac{\omega_k}{2k_B T}\right) \left(\frac{\Delta_k}{\omega_k}\right)^2 & (\delta(\omega - 2\omega_k) \\ - \delta(\omega + 2\omega_k)), & \end{aligned} \quad (24)$$

where

$$C(\theta_I, \theta_S) = \frac{1}{4} \left[\gamma_{\perp} \sin\theta_I \sin\theta_S - \frac{\gamma_{\parallel} J_{\perp}}{J_{\parallel}} \cos\theta_I \cos\theta_S \right]. \quad (25)$$

It measures, up to a matrix element, the density of states of the triplet excitations. The Raman scattering spectra thus displays two peaks at its edges, the first one at energy $\omega = 2\omega_{\pi} = 2\Delta_s$ corresponding to the bottom of the triplet band, and the second one at $\omega = 2\omega_0$, corresponding to the top of the triplet band. Such peaks have been observed experimentally^{15,14,13,12}. Within mean field theory, it is possible to consider the effect of a non-zero temperature. For $J_{\perp}/J = 10$ the temperature effect is negligible as long as $T < 0.5J_{\perp}$. For larger T , there is a decrease of s that causes a decrease of the bandwidth of triplet excitations (see Fig. 4). The effect of $C(\theta_I, \theta_S)$ is to give an explicit dependence on the polarization of incoming and outgoing radiation to the Raman intensity. However, it does not give rise to a shift of the peaks when the polarization is changed. In the case $\gamma_{\perp}/\gamma_{\parallel} = J_{\perp}/J_{\parallel}$, the Raman intensity is proportional to $\cos^2(\theta_I + \theta_S)$ as pointed out in Ref. 34.

Eq. (24) was derived neglecting triplet-triplet scattering. Such scattering is responsible for the broadening of the peaks in experiments^{15,14,13,12}. A full calculation of the effect of triplet-triplet scattering is a very complex task. Physically, the most important effect of these interactions is that triplet bosons are not anymore exact eigenstates of the Hamiltonian and acquire a finite lifetime τ . An estimate of this lifetime is given by the Fermi Golden rule as:

$$\begin{aligned} \frac{1}{\tau} = 2\pi \sum_{k',q} |V(q)|^2 n_B(k') (1 + n_B(k' + q)) \\ \times \delta(\epsilon(k+q) + \epsilon(k-q) - \epsilon(k) - \epsilon(k')). \end{aligned} \quad (26)$$

The potential for triplet-triplet interactions being short ranged, $V(q) \simeq V(q=0) = V_0$. Since the quasi-particle dispersion is of the form: $\omega_k = \omega_{\pi} + \frac{k^2}{2m_{\pi}}$ at the bottom of the spectrum, $\frac{1}{\tau}$ will be dominated by a factor

$e^{-\omega_\pi/T}$. The rest of the expression reduces to a phase space factor, independent of temperature.

The existence of a finite lifetime for the quasiparticles leads to the replacement

$$\delta(\omega - 2\omega_k) \rightarrow \frac{\Gamma}{\pi} \frac{1}{(\omega - 2\omega_k)^2 + \Gamma^2}, \quad (27)$$

in Eq. 24. At temperatures $T \ll \omega_0$, Γ is small and such replacement does not affect the intensity very much except at the edges where it cuts the square root singularities of the density of states. Thus, we can restrict to the consideration of Raman intensity close to the edges of the spectrum.

Let us first consider the threshold $\omega \sim \omega_\pi$. The Raman intensity is approximately:

$$\begin{aligned} I(\omega) &= \coth\left(\frac{\omega_\pi}{k_B T}\right) \left(\frac{\Delta_\pi}{\omega_\pi}\right)^2 \int \frac{dk}{2\pi} \frac{\Gamma_\pi}{\pi} \frac{1}{(\omega - 2\omega_\pi - \frac{k^2}{m_\pi})^2 + \Gamma_\pi^2} \\ &= \coth\left(\frac{\omega_\pi}{k_B T}\right) \left(\frac{\Delta_\pi}{\omega_\pi}\right)^2 \tilde{I}(\omega) \end{aligned} \quad (28)$$

where

$$m_\pi = \frac{2\sqrt{1-d}}{d\left(\frac{J_\perp}{4} - \mu\right)} \quad (29)$$

The calculation leads to:

$$\tilde{I}(\omega) = \frac{\sqrt{\frac{m_\pi \Gamma_\pi^2}{8\pi^2}}}{\sqrt{(\omega - 2\Delta)^2 + \Gamma_\pi^2} \sqrt{\sqrt{(\omega - 2\Delta)^2 + \Gamma_\pi^2} - \omega + 2\Delta}} \quad (30)$$

The resulting plot of $I(\omega)$ versus ω is shown on figure 5 and is qualitatively similar to the behavior of the Raman intensity close to $2\Delta_s$ in experimental systems (see Fig. 3 in Ref. 13 or Fig. 5 in Ref. 15). Eq. (30) can be cast in the scaling form:

$$\tilde{I}(\omega) = \sqrt{\frac{8\pi^2 \Gamma_\pi}{m_\pi}} I_{1D}(\omega) = \frac{1}{\sqrt{x^2 + 1} \sqrt{\sqrt{x^2 + 1} - x}}, \quad (31)$$

where $x = \frac{\omega - 2\Delta}{\Gamma_\pi}$. The corresponding plot is Fig. 6. It would be interesting to determine whether the experimental data satisfy such scaling form. A similar calculation can be done for $\omega \sim \omega_0$, with result:

$$I(\omega) = \coth\left(\frac{\omega_0}{2k_B T}\right) \left(\frac{\Delta_0}{\omega_0}\right)^2 \sqrt{\frac{m_0}{8\pi^2 \Gamma_0}} I_{1D}\left(\frac{2\omega_0 - \omega}{\Gamma_0}\right) \quad (32)$$

where:

$$m_0 = \frac{2\sqrt{1+d}}{d\left(\frac{J_\perp}{4} - \mu\right)} \quad (33)$$

Although in experiments on $\text{Sr}_{14}\text{Cu}_{24}\text{O}_{41}$ the condition $J_\perp \gg J$ is certainly not satisfied, it is nevertheless

interesting to compare the dependence predicted by Eq. (32) with the two magnon intensity of Fig. 4 in 15 or Fig. 7 of Ref. 16. At temperatures small in comparison to the spin gap, the damping effect is the dominant feature near the edges. At low temperature there is a rapid variation of the damping rate $\Gamma = 1/\tau \sim e^{-\Delta_s/T}$ with temperature and thus a rapid variation of the intensity. It would be interesting to check whether such dependence of the damping rate is consistent with experiments. As a final note, we would like to point out that Equations (30) and (32) do not lead in general to a symmetric Raman spectra. In particular, in the case of CaV_2O_5 , a different damping rate and different masses of excitations could explain the difference of behavior of the intensity at the two edges¹³.

III. COUPLED LADDERS

A. Mean field equations

In this section we start to consider the effects on the Raman intensity due to interladder interaction. Our final aim is to derive an expression of the Raman intensity in the case of the array of ladders whose Hamiltonian was given in Eq. (1). Such ladder array model is of interest for systems such as KCuCl_3 ²⁶ or possibly CuHpCl ²⁸ according to some neutron scattering experiments. As a simpler problem, we will also discuss a double rung ladder in which two spin-1/2 ladders are connected by interladder exchange of strength $\lambda' J_\perp$, that is weaker than the intraladder coupling. In the BOT the Hamiltonian given by Eq. 14 where the index j can run now from 1 to N. First we apply the Green's function method to determine the spectrum, whose complete calculation is reported in the Appendix . It will be given by

$$\begin{aligned} \omega^2(k_x, k_y) &= \left(\frac{J_\perp}{4} - \mu - J_\parallel s^2 \cos(k_x) + \frac{\lambda' J_\perp s^2}{2} \cos(k_y)\right)^2 \\ &\quad - \left(J_\parallel s^2 \cos(k_x) - \frac{\lambda' J_\perp s^2}{2} \cos(k_y)\right)^2. \end{aligned} \quad (34)$$

The self-consistent equations in the saddle-point approximation that permit us to determine the parameters (s^2, μ) at $T=0$ are given by

$$\left(s^2 - \frac{3}{2}\right) + \int_{-\pi/a}^{\pi/a} \frac{dk_x}{(2\pi)} \int_{-\pi/a}^{\pi/a} \frac{dk_y}{(2\pi)} \left[\frac{1 - \frac{d}{2} f(k_x, k_y)}{\sqrt{1 - df(k_x, k_y)}} \right] = 0 \quad (35)$$

$$\left(\frac{3}{2} + 2\frac{\mu}{J_\perp}\right) + \lambda \int_{-\pi/a}^{\pi/a} \frac{dk_x}{(2\pi)} \int_{-\pi/a}^{\pi/a} \frac{dk_y}{(2\pi)} \left[\frac{f(k_x, k_y)}{\sqrt{1 - df(k_x, k_y)}} \right] = 0 \quad (36)$$

where

$$d = \frac{\lambda s^2}{\left(\frac{1}{4} - \frac{\mu}{J_\perp}\right)} \quad (37)$$

$$f = \left(\frac{2\lambda}{\lambda'} \cos k_x - \cos k_y\right) \quad (38)$$

Note that the two coupled ladders case is included in the formula above since we can restrict the sum over k_y to 0 and π . The expression (46) is very general and contains an explicit dependence on the polarization and the electric field intensity. We emphasize that the peak position predicted by Eq. (46) only depends on the spectrum of the ladder system. In particular, it is completely independent of the polarization of ingoing as well as outgoing radiation.

Performing an analytic continuation, the intensity of the Raman spectrum is given by

$$\text{Im}\chi_R(\omega) = \int \int \frac{d^2k}{(2\pi)^2} M_{\mathbf{k}} (\delta(\omega - 2\omega_{\mathbf{k}}) - \delta(\omega + 2\omega_{\mathbf{k}})), \quad (50)$$

where $M_{\mathbf{k}}$ is given by (48). Since the γ 's appearing in the expression for $M_{\mathbf{k}}$ can be treated as phenomenological parameters we will perform the explicit calculation for $\gamma_{\parallel}/J_{\parallel} = \gamma_{\perp}/J_{\perp} = \gamma'_{\perp}/J'_{\perp}$.

1. The Raman intensity of the two-rung ladder

Using the previous formulas, the Raman intensity for the two-rung ladder will be obtained from formula (50) reducing the integral on k_y to a sum for $k_y = 0$ and $k_y = \pi$:

$$\text{Im}\chi_R(\omega) = \sum_{\alpha=1,2} \int dk \left(\frac{A_k^2 (\Lambda_k \Delta_k - \Delta_k^2)}{\omega_{k,\alpha}^2} \right) (\delta(\omega - 2\omega_{k,\alpha}) - \delta(\omega + 2\omega_{k,\alpha})). \quad (51)$$

Here we have summed on the two triplet bands. Performing the integral in (51), we obtain as a final result

$$\text{Im}\chi_R(\omega) = A_0 \sum_{\alpha=\pm} \frac{\left| \left(\frac{\omega}{2(J_{\perp}/4 - \mu)} \right)^2 - a_{\alpha} \right|^3 \left[1 + \frac{1}{4} \left[\left(\frac{\omega}{2(J_{\perp}/4 - \mu)} \right)^2 - a_{\alpha} \right] \right]}{4\omega \sqrt{\left(\frac{2J_S^2}{J_{\perp}/4 - \mu} \right)^2 - \left[\left(\frac{\omega}{2(J_{\perp}/4 - \mu)} \right)^2 - a_{\alpha} \right]^2}}, \quad (52)$$

$$I_{2D}^{\text{edge}}(\omega) = \int \frac{kdk}{2\pi} \frac{\Gamma}{(\omega - 2\Delta - k^2)^2 + \Gamma^2} = \frac{2}{\pi^2} \left(\frac{\pi}{2} + \arctan \frac{\omega - 2\Delta}{\Gamma} \right). \quad (55)$$

where $A_0 = (J_{\perp}/4 - \mu)^3 \left(\frac{\gamma_{\parallel}}{J_{\parallel}} \right)^2 \cos^2(\theta_I + \theta_S)$, $a_{\pm} = (1 \pm \frac{1}{2} \frac{\lambda'}{\lambda})$. As shown in Fig.7, the Raman spectrum shows four peaks in correspondence of the bottom and the top the bonding and antibonding bands. From simple density of states argument, no signal should be seen for $\omega < 2\Delta_s$, where Δ_s is the singlet-triplet gap.

2. The array of ladders

In this case we start from equation (50), by introducing the two-dimensional density of states $\rho(\omega)$ and we can write

$$\text{Im}\chi_R(\omega) \propto \frac{1}{4} \rho(\omega/2) \left[\left(\frac{\omega}{2(J_{\perp}/4 - \mu)} \right)^2 - 1 \right], \quad (53)$$

$$\rho(\omega) = \frac{2}{\pi} \left[\frac{\omega}{(J_{\perp}/4 - \mu)} \right] \frac{1}{J_{\parallel} s^2} \int \frac{dk_y}{2\pi} \frac{1}{\sqrt{1 - \left(\frac{1}{d} \left(1 - \left(\frac{\omega}{(J_{\perp}/4 - \mu)} \right)^2 \right) + \frac{\lambda'}{2\lambda} \cos k_y \right)^2}}. \quad (54)$$

The last integral is performed for $Max(-1, +\frac{2\lambda}{2\lambda'}) - \frac{2\lambda}{d\lambda'} \left(1 - \left(\frac{\omega}{(J_{\perp}/4 - \mu)} \right)^2 \right) < \cos k_y < Min(1, -\frac{2\lambda}{\lambda'} - \frac{2\lambda}{d\lambda'} \left(1 - \left(\frac{\omega}{(J_{\perp}/4 - \mu)} \right)^2 \right))$. The results show that the intensity is non-zero only between the maximum and the minimum of $\omega(\mathbf{k})$ and a discontinuity appears at the band edge. The behavior of the 2D Raman intensity is sketched on Fig. 8.

In two dimensions, we can expect two types of singularities in $\rho(\omega)$, namely discontinuities and logarithmic singularities³⁵. Close to these singularities, damping effects due to triplet-triplet scattering will play an important role, in analogy to the single ladder problem. In the present case the two-magnon continuum starts at energy: $\omega_- = 2\Delta_s = 2(J_{\perp}/4 - \mu) \sqrt{1 - d(1 + \frac{\lambda'}{2\lambda})}$, the other edge of the Raman spectrum being at $\omega_+ = 2(J_{\perp}/4 - \mu) \sqrt{1 + d(1 + \frac{\lambda'}{2\lambda})}$. No magnetic Raman scattering is observed for $\omega \notin [\omega_-, \omega_+]$. At these points, discontinuities in the Raman intensity would appear in the absence of damping. Taking damping into account close to the edges of the spectrum, we find that the intensity is of the form:

The steps at the edges of the spectrum are thus smoothed out by damping of excitations. The corresponding plot is Fig. 9.

At a logarithmic singularity $\omega \sim 2(J_{\perp}/4 - \mu) \sqrt{1 \pm d(1 - \frac{\lambda'}{2\lambda})}$, we find that:

$$I_{2D}^{\text{peak}}(\omega) = \int \frac{dk_x dk_y}{(2\pi)^2} \frac{\Gamma}{\pi} \frac{1}{(\omega - 2\Delta - k_x^2/m + k_y^2/m)^2 + \Gamma^2}, \quad (56)$$

and thus:

$$I(\omega) \sim \ln \frac{\Lambda^2}{\Gamma^2 + (\omega - 2\Delta)^2}, \quad (57)$$

where Λ is an energy cutoff. Again, the height of the peaks is limited by the damping of excitations. Note that in contrast to the one dimensional case, the peaks are not obtained at the edges of the two magnon Raman spectrum but are superposed onto a positive two-magnon background. Only in the one dimensional limit do the peaks merge with the steps at the edge of the spectrum. Also, in the two dimensional case, the peaks are symmetric (see Fig. 10) in contrast to the 1D case. Thus, Raman scattering can prove useful to discriminate quasi-one dimensional systems from quasi two-dimensional systems with a spin gap^{28,30} and provide bounds on interladder coupling.

IV. CONCLUSION

We have presented an analysis of the Raman spectra for various coupled spin ladder systems based on the Loudon-Fleury photon-induced super-exchange theory, representing the spins using the Bond Operator Formalism. For a single ladder, we have shown that peaks should appear at the edges of the Raman spectrum as has been observed in experiments^{13,16}. The shape of these peaks is determined by the damping of triplet excitations due to interactions. A scaling plot of the Raman intensity versus frequency should permit to determine the lifetime of excitations in the ladder. Simple arguments lead us to expect that the lifetime of excitations must vary as $e^{\Delta/T}$ where Δ is the spin gap. Another consequence of a positive temperature on the spin ladder is the narrowing of the spectrum as temperature is increased. It would be interesting to compare our predictions to the available experimental data on spin ladder systems. In the case of the coupled array of ladders, we have shown that the Raman scattering intensity measures the density of states of triplet excitations. Thus, the singularities of the Raman intensity should indicate very clearly whether the system is one or two dimensional. In both case, the peak position was independent from the polarization of the incoming and scattered radiation. It would be interesting to generalize our analysis to other two dimensional spin gap systems such as the models with orthogonal dimers³⁶ that can be used to model $\text{SrCu}_2(\text{BO}_3)_2$. Another direction in which our work could be extended is to conducting spin ladders¹⁵ in which case charge degrees of freedom could also come into play.

ACKNOWLEDGMENTS

We thank G. Blumberg, R. Chitra, T. Giamarchi and C. M. Varma for illuminating discussions. E. O. acknowledges partial support from NSF under grants DMR 96-14999 and DMR 99-76665. R. Citro acknowledges support from INFM and thanks Laboratoire de Physique

Théorique de l'École Normale Supérieure for kind hospitality.

APPENDIX: GREEN'S FUNCTIONS METHOD FOR THE ARRAY OF LADDERS

We introduce the following Green's functions:

$$\begin{aligned} G_\alpha(\mathbf{k}, \tau) &= -\langle T_\tau t_{\mathbf{k},\alpha}(\tau) t_{\mathbf{k},\alpha}^\dagger(0) \rangle \\ \tilde{G}_\alpha(\mathbf{k}, \tau) &= -\langle T_\tau t_{\mathbf{k},\alpha}^\dagger(\tau) t_{\mathbf{k},\alpha}(0) \rangle \\ F_\alpha(\mathbf{k}, \tau) &= -\langle T_\tau t_{\mathbf{k},\alpha}(\tau) t_{-\mathbf{k},\alpha}(0) \rangle \\ (F^\dagger)_\alpha(\mathbf{k}, \tau) &= -\langle T_\tau t_{\mathbf{k},\alpha}^\dagger(\tau) t_{\mathbf{k},\alpha}^\dagger(0) \rangle \end{aligned} \quad (\text{A1})$$

The equations of motion permit us to obtain the following coupled equations:

$$\begin{aligned} -i\omega_n G_\alpha(\mathbf{k}, \omega_n) &= -1 - \left(\frac{J_\perp}{4} - \mu \right) G_\alpha(\mathbf{k}, \omega_n) \\ -s^2 \left(J_\parallel \cos(k_x) - \frac{\lambda' J_\perp}{2} \cos(k_y) \right) &[G_\alpha(\mathbf{k}, \omega_n) + F_\alpha^\dagger(\mathbf{k}, \omega_n)] \\ -i\omega_n F_\alpha^\dagger(\mathbf{k}, \omega_n) &= \left(\frac{J_\perp}{4} - \mu \right) F_\alpha^\dagger(\mathbf{k}, \omega_n) \\ +s^2 \left(J_\parallel \cos(k_x) - \frac{\lambda' J_\perp}{2} \cos(k_y) \right) &[G_\alpha(\mathbf{k}, \omega_n) + F_\alpha^\dagger(\mathbf{k}, \omega_n)] \end{aligned} \quad (\text{A2})$$

and:

$$\begin{aligned} -i\omega_n \tilde{G}_\alpha(\mathbf{k}, \omega_n) &= 1 + \left(\frac{J_\perp}{4} - \mu \right) G_\alpha(\mathbf{k}, \omega_n) \\ +s^2 \left(J_\parallel \cos(k_x) - \frac{\lambda' J_\perp}{2} \cos(k_y) \right) &[\tilde{G}_\alpha(\mathbf{k}, \omega_n) + F_\alpha(\mathbf{k}, \omega_n)] \\ -i\omega_n F_\alpha(\mathbf{k}, \omega_n) &= -\left(\frac{J_\perp}{4} - \mu \right) F_\alpha^\dagger(\mathbf{k}, \omega_n) \\ -s^2 \left(J_\parallel \cos(k_x) - \frac{\lambda' J_\perp}{2} \cos(k_y) \right) &[\tilde{G}_\alpha(\mathbf{k}, \omega_n) + F_\alpha(\mathbf{k}, \omega_n)] \end{aligned} \quad (\text{A3})$$

It is convenient to introduce:

$$\Lambda(\mathbf{k}) = \frac{J_\perp}{4} - \mu + J_\parallel s^2 \cos(k_x) - \frac{J'_\perp s^2}{2} \cos(k_y) \quad (\text{A4})$$

and:

$$2\Delta(\mathbf{k}) = J_\parallel s^2 \cos(k_x) - \frac{J'_\perp s^2}{2} \cos(k_y) \quad (\text{A5})$$

so that:

$$\begin{aligned} G(\mathbf{k}, \omega_n) &= (\tilde{G}(\mathbf{k}, \omega_n))^* = -\frac{i\omega_n + \Lambda(\mathbf{k})}{\omega_n^2 + \omega(\mathbf{k})^2} \\ F(\mathbf{k}, \omega_n) &= F^\dagger(\mathbf{k}, \omega_n) = \frac{2\Delta_k}{\omega_n^2 + \omega(\mathbf{k})^2} \end{aligned} \quad (\text{A6})$$

Where we have:

$$\omega^2(\mathbf{k}) = \Lambda^2(\mathbf{k}) - (2\Delta(\mathbf{k}))^2 \quad (\text{A7})$$

The dispersion for the isolated ladder is obtained by taking $J'_\perp = 0$ in the preceding formulas.

A convenient decomposition of the Green's functions is:

$$G(\mathbf{k}, \omega_n) = \frac{1}{2} \left[\left(1 + \frac{\Lambda(\mathbf{k})}{\omega(\mathbf{k})}\right) \frac{1}{i\omega_n + \omega(\mathbf{k})} + \left(1 - \frac{\Lambda(\mathbf{k})}{\omega(\mathbf{k})}\right) \frac{1}{i\omega_n - \omega(\mathbf{k})} \right]$$

$$F^\dagger(k, \omega_n) = \frac{\Delta(\mathbf{k})}{\omega(\mathbf{k})} \left[\frac{1}{i\omega_n + \omega(\mathbf{k})} - \frac{1}{i\omega_n - \omega(\mathbf{k})} \right] \quad (\text{A8})$$

Using this decomposition, the Matsubara sums are reduced to:

$$\frac{1}{\beta} \sum_{\nu_n} \frac{1}{i(\omega_n + \nu_n) \pm \omega(\mathbf{k})} \frac{1}{i\omega_n \pm \omega(\mathbf{k})} = 0 \quad (\text{A9})$$

$$\frac{1}{\beta} \sum_{\nu_n} \frac{1}{i(\omega_n - \nu_n) \pm \omega(\mathbf{k})} \frac{1}{i\omega_n \mp \omega(\mathbf{k})} = \pm \frac{\coth\left(\frac{\beta\omega_{\mathbf{k}}}{2}\right)}{i\nu_n \mp 2\omega_{\mathbf{k}}} \quad (\text{A10})$$

$$(\text{A11})$$

with the appropriate factor.

This gives us the following integrals:

$$\begin{aligned} & \frac{1}{\beta} \sum_{i\nu_n} G_{\mathbf{k}}(i\nu_n) G_{\mathbf{k}}(i\nu_n - i\omega_n) = \\ & - \left(\frac{\Delta_{\mathbf{k}}}{\omega_{\mathbf{k}}}\right)^2 \coth\left(\frac{\beta\omega_{\mathbf{k}}}{2}\right) \left[\frac{1}{i\omega_n - 2\omega_{\mathbf{k}}} - \frac{1}{i\omega_n + 2\omega_{\mathbf{k}}} \right] \\ & \frac{1}{\beta} \sum_{i\nu_n} F_{\mathbf{k}}(i\nu_n) F_{\mathbf{k}}(i\nu_n - i\omega_n) = \\ & - \left(\frac{\Delta_{\mathbf{k}}}{\omega_{\mathbf{k}}}\right)^2 \coth\left(\frac{\beta\omega_{\mathbf{k}}}{2}\right) \left[\frac{1}{i\omega_n - 2\omega_{\mathbf{k}}} - \frac{1}{i\omega_n + 2\omega_{\mathbf{k}}} \right] \\ & \frac{1}{\beta} \sum_{i\nu_n} [F_{\mathbf{k}}(i\nu_n) G_{\mathbf{k}}(i\nu_n - i\omega_n) + G_{\mathbf{k}}(i\nu_n) F_{\mathbf{k}}(i\nu_n - i\omega_n)] \\ & = \frac{\Delta_{\mathbf{k}} \Lambda_{\mathbf{k}}}{\omega_{\mathbf{k}}^2} \coth\left(\frac{\beta\omega_{\mathbf{k}}}{2}\right) \left[\frac{1}{i\omega_n - 2\omega_{\mathbf{k}}} - \frac{1}{i\omega_n + 2\omega_{\mathbf{k}}} \right] \\ & \frac{1}{\beta} \sum_{i\nu_n} G_{\mathbf{k}}(i\nu_n) [G_{\mathbf{k}}(i\nu_n - i\omega_n) + G_{\mathbf{k}}(-i\nu_n + i\omega_n)] \\ & = \left(\frac{\Delta_{\mathbf{k}}}{\omega_{\mathbf{k}}}\right)^2 \coth\left(\frac{\beta\omega_{\mathbf{k}}}{2}\right) \left[\frac{1}{i\omega_n + 2\omega_{\mathbf{k}}} - \frac{1}{i\omega_n - 2\omega_{\mathbf{k}}} \right] \quad (\text{A12}) \end{aligned}$$

This allows the complete calculation of the Raman intensity. For instance, in the single rung case, the intensity is given by:

$$\chi_R(i\omega_n) = \frac{1}{\beta} C^2(\theta_I, \theta_S) \sum_{\nu_n} \int \frac{dk}{2\pi} [G(k, i\nu_n) G(k, i\nu_n - i\omega_n) + F(k, i\nu_n) F^\dagger(k, i\omega_n - i\nu_n)], \quad (\text{A13})$$

where $C(\theta_I, \theta_S)$ is given by Eq. (25).

Using Eqs. (A12) one obtains the expression Eq. (24) for the Raman intensity.

-
- ¹ E. Dagotto and T. M. Rice, *Science* **271**, 618 (1996), and references therein.
 - ² D. Johnston *et al.*, *Magnetic Susceptibilities of Spin-1/2 Antiferromagnetic Heisenberg Ladders and Applications to Ladder Oxide Compounds*, cond-mat/0001147, 2000.
 - ³ I. Yamada and H. Onda, *Phys. Rev. B* **49**, 1048 (1994).
 - ⁴ P. E. Sulewski and S.-W. Cheong, *Phys. Rev. B* **51**, 3021 (1995).
 - ⁵ P. Lemmens *et al.*, *Physica B* **223–224**, 535 (1996).
 - ⁶ P. van Loosdrecht, in *Contemporary studies in condensed matter physics*, Vol. 61-62 of *Solid State phenomena*, edited by M. Davidovic and Z. Ikonic (Scitec, Switzerland, 1998), p. 19, cond-mat/9711091.
 - ⁷ H. Kuroe *et al.*, *J. Phys. Soc. Jpn.* **67**, 2881 (1998), cond-mat/9805251.
 - ⁸ S. A. Golubchik *et al.*, *J. Phys. Soc. Jpn.* **66**, 4042 (1997), cond-mat/9711048.
 - ⁹ G. S. Uhrig and H. J. Schulz, *Phys. Rev. B* **54**, R9624 (1996).
 - ¹⁰ W. Brenig, *Phys. Rev. B* **56**, 2551 (1997), cond-mat/9702210.
 - ¹¹ D. Augier, E. Sorensen, J. Riera, and D. Poilblanc, *Phys. Rev. B* **60**, 1075 (1999).
 - ¹² M. V. Abrashev, C. Thomsen, and M. Surtchev, *Physica C* **280**, 297 (1997).
 - ¹³ M. J. Konstantinović, Z. V. Popović, M. Isobe, and Y. Ueda, *Phys. Rev. B* **61**, 15185 (2000), cond-mat/0001168.
 - ¹⁴ S. Sugai *et al.*, *Phys. Rev. B* **60**, R6969 (1999).
 - ¹⁵ S. Sugai and M. Suzuki, *Phys. Stat. Sol. (b)* **215**, 653 (1999).
 - ¹⁶ Z. V. Popović *et al.*, cond-mat/0005096 (unpublished).
 - ¹⁷ Y. Natsume, Y. Watabe, and T. Suzuki, *J. Phys. Soc. Jpn.* **67**, 3314 (1998).
 - ¹⁸ E. Orignac and R. Citro, *Phys. Rev. B* **62**, 8622 (2000), cond-mat/0002257.
 - ¹⁹ P. A. Fleury and R. Loudon, *Phys. Rev.* **166**, 514 (1968).
 - ²⁰ T. Moriya, *J. Applied Phys.* **39**, 42 (1968).
 - ²¹ B. S. Shastry and B. I. Shraiman, *Phys. Rev. Lett.* **65**, 1068 (1990).
 - ²² D. G. Shelton, A. A. Nersesyan, and A. M. Tsvelik, *Phys. Rev. B* **53**, 8521 (1996).
 - ²³ A. V. Chubukov, *JETP Lett.* **49**, 129 (1989).
 - ²⁴ S. Sachdev and R. N. Bhatt, *Phys. Rev. B* **41**, 9323 (1990).
 - ²⁵ S. Gopalan, T. M. Rice, and M. Sigrist, *Phys. Rev. B* **49**, 8901 (1994).
 - ²⁶ N. Cavadini *et al.*, *Eur. Phys. J. B* **7**, 519 (1999).
 - ²⁷ A. W. Garrett *et al.*, *Phys. Rev. Lett.* **79**, 745 (1997).
 - ²⁸ P. H. Hammar, D. H. Reich, C. Broholm, and F. Trouw, *Phys. Rev. B* **57**, 7846 (1998).
 - ²⁹ G. Chaboussant *et al.*, *Phys. Rev. B* **55**, 3046 (1997).

- ³⁰ G. Chaboussant *et al.*, Phys. Rev. Lett. **80**, 2713 (1998).
³¹ G. Chaboussant *et al.*, Eur. Phys. J. B **6**, 167 (1998).
³² R. Loudon, J. Phys. C **3**, 872 (1970).
³³ G. F. Reiter, Phys. Rev. B **13**, 169 (1976).
³⁴ P. J. Freitas and R. R. P. Singh, cond-mat/0004477 (unpublished).
³⁵ J. M. Ziman, *Principles of the Theory of Solids* (Cambridge University Press, Cambridge, 1972).
³⁶ K. Ueda and S. Miyahara, J. Phys.: Condens. Matter **11**, L175 (1999).

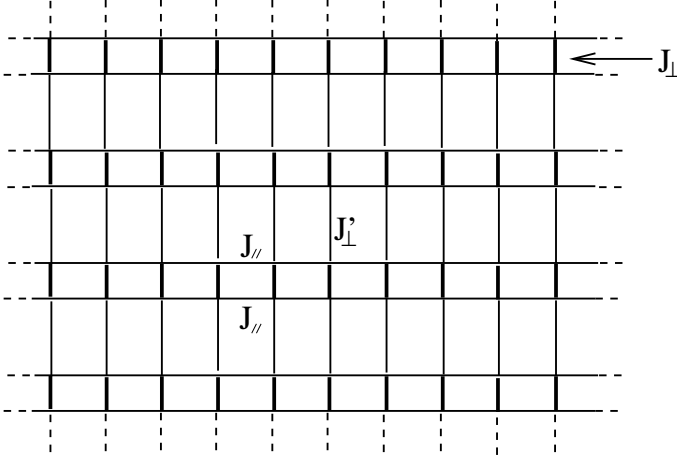


FIG. 1. The two dimensional array of ladders.

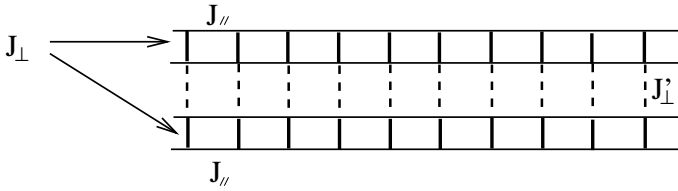


FIG. 2. The double ladder

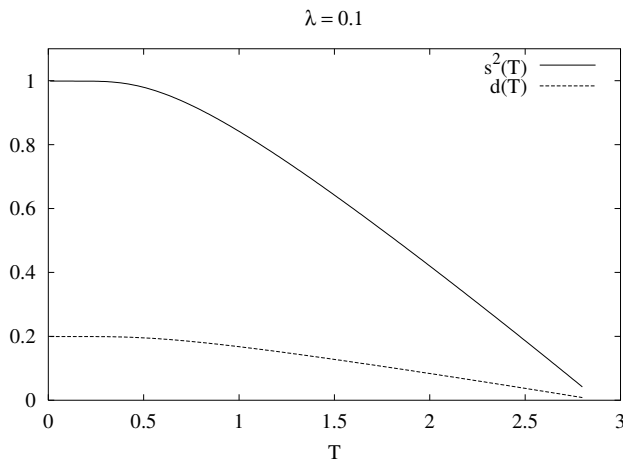


FIG. 3. The singlet order parameter $s^2(T)$ and $d^2(T)$ as a function of the temperature (in units of J_{\perp}) for $\lambda = 0.1$.

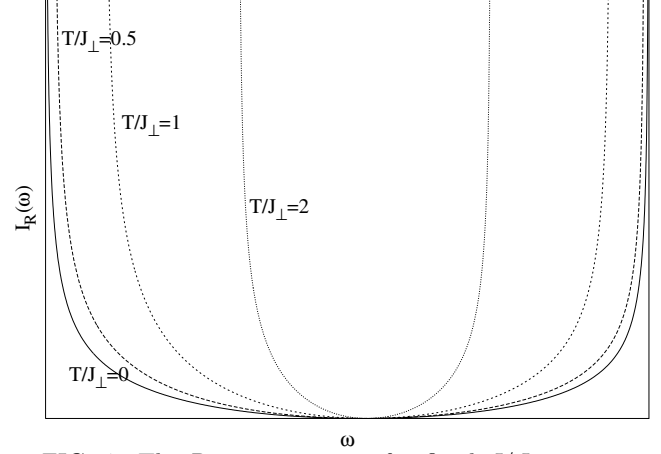


FIG. 4. The Raman intensity for fixed $J/J_{\perp} = 0.1$ and increasing T/J_{\perp} . For $T/J_{\perp} < 0.1$ the effect of temperature on the Raman intensity is not visible. For $T/J_{\perp} > 0.5$, the peaks are moving toward each other as a consequence of the diminution of s and Δ

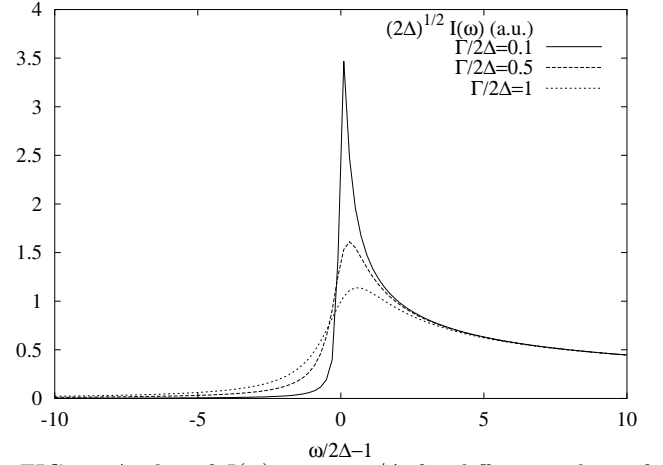


FIG. 5. A plot of $I(\omega)$ versus ω/Δ for different values of Γ/Δ . Increasing temperature amounts to increasing Γ and results in a reduction of peak intensity and the apparition of a small intensity below the gap

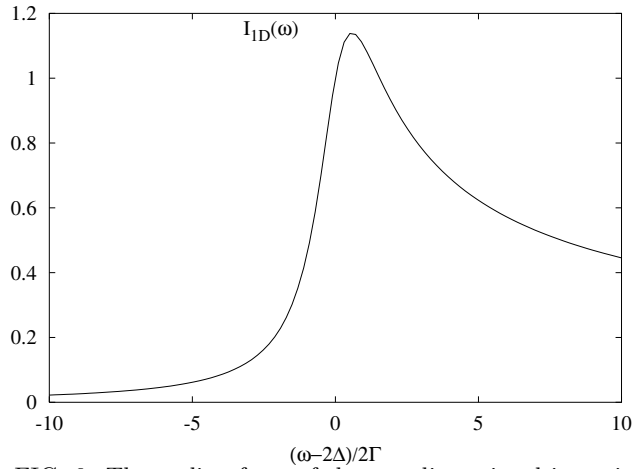


FIG. 6. The scaling form of the one dimensional intensity Eq. (30)

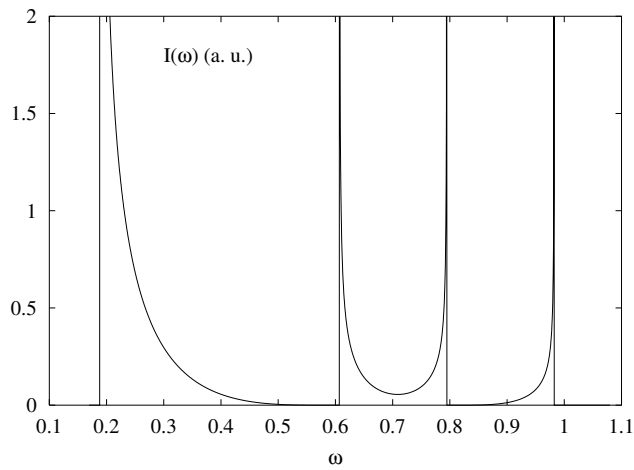


FIG. 7. Raman intensity for the two coupled ladders, for $J/J_{\perp} = 0.3$, $J'/J_{\perp} = 0.1$.

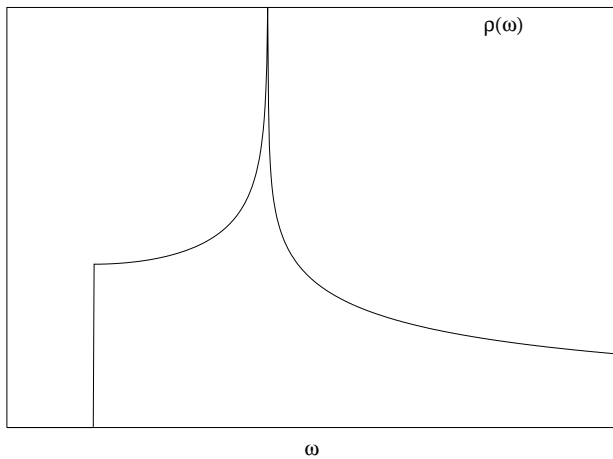


FIG. 8. The behavior of the density of states in a two dimensional system, showing a discontinuity at threshold and a logarithmic peak inside the spectrum.

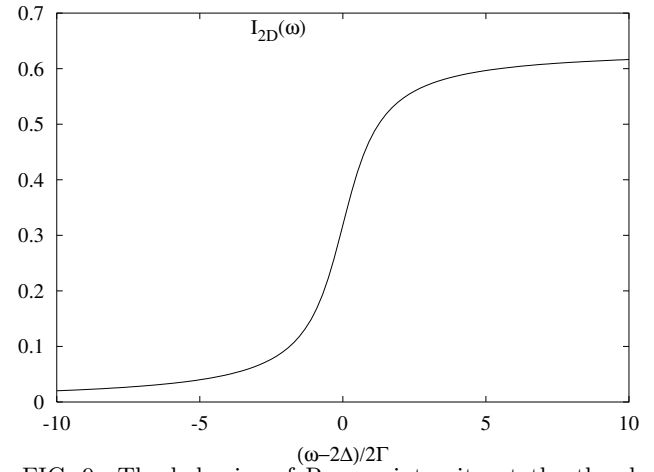


FIG. 9. The behavior of Raman intensity at the threshold of the two-magnon spectrum in a two dimensional ladder array taking into account the damping of triplet excitations.

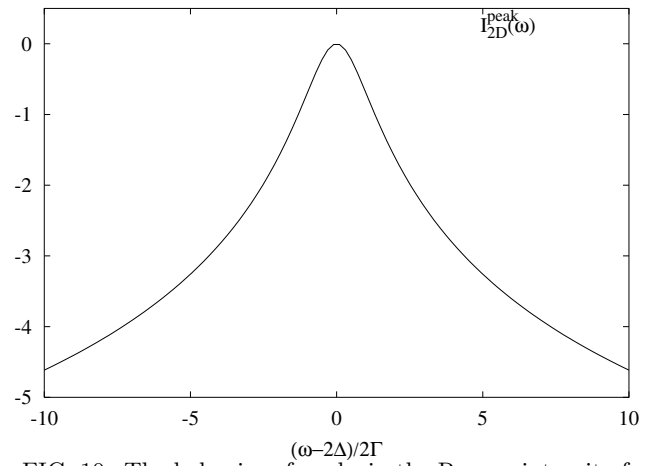


FIG. 10. The behavior of peaks in the Raman intensity for a two dimensional array with damping of triplet excitation taken into account. Note the symmetry of the spectrum, to be contrasted with Fig. 6.